Yaw Stability Control of Vehicles Using a Slip Polytope Validated with Real Tests

Yaw Stability Control of Vehicles Using a Slip Polytope Validated with Real Tests

Umur Erdinc[1,2(✉)], Mats Jonasson[2], Maliheh Sadeghi Kati[1], Leo Laine[1,2], Bengt Jacobson[2], and Jonas Fredriksson[2]

[1] Volvo Group Trucks Technology, Gothenburg, Sweden
umur.erdinc@volvo.com
[2] Chalmers University of Technology, Gothenburg, Sweden

Abstract. Articulated heavy vehicles (AHVs) face yaw instabilities, especially under extensive propulsion or regenerative braking force on the driven axles, risking their directional stability and potentially leading to jackknifing. Hence, safe operating envelopes (SOEs) are essential for allocating propulsion and braking forces among different units. This study proposes a novel approach to ensure yaw stability by reducing longitudinal slip limits of the electric motors (EMs) based on side-slip, enhancing stability and acceleration performance. Validation through simulations and real vehicle tests shows promising results.

Keywords: Safe Operating Envelope · Slip Polytope · Jackknifing · Articulated Heavy Vehicles · Slip Controller · Yaw Stability

1 Introduction

Electrification affects both trucks and trailing units like trailers and dollies. With multiple units propelled, AHVs face increased risk of yaw instabilities. Regenerative braking by tractor's EMs without braking semitrailer can cause jackknifing, while braking only semitrailer's EMs with an unbraked tractor can lead to trailer swing [1]. The same problems may also occur during propulsion. Hence, safe motion control of AHVs is crucial while maintaining the highest energy efficiency. While previous research defines SOEs in wheel force domain [1, 2], side-slip angle vs. side-slip angle rate [3], lateral velocity vs. yaw rate [4] or side-slip angle vs. yaw rate [5], this study forms a SOE in the longitudinal slip vs. side-slip angle domain. Advanced EMs in modern AHVs offer new opportunities for ensuring yaw stability. While slip controllers usually have rather constant longitudinal slip limits, it is a well-known fact in vehicle dynamics that high longitudinal slip reduces lateral force generation for a given lateral slip [6]. Thus, an advanced slip control strategy, rather than fixed slip limits, is needed to ensure yaw stability.

This study investigates an electric tractor and conventional semitrailer combination, introducing a new slip control strategy. Longitudinal slip limits of EMs vary based on side-slip angle deviation from an estimated reference value at the driven axle. This approach ensures adequate lateral force capability and yaw stability, tested first through

G. Mastinu et al. (Eds.): AVEC 2024, LNME, pp. 130–136, 2024.
https://doi.org/10.1007/978-3-031-70392-8_19

simulations, and then validated with a real test vehicle on a circular snow/ice test track, at Colmis Proving ground in Northern Sweden.

2 Reference Side-Slip Ange Estimation

A reference side-slip angle for the vehicle is obtained with an estimator incorporating a single-track vehicle model. The free-body diagram of the tractor is shown in Fig. 1. The lateral force and the yaw moment equilibria around the center of gravity (CoG) for the tractor are expressed as:

$$\begin{aligned} m_1 \cdot \left(\dot{v}_{1y} + \omega_{1z} \cdot v_{1x}\right) &= \cos\left(\delta_f\right) \cdot F_{1fyw} + F_{1ry} + P_{1cy} \\ J_1 \cdot \dot{\omega}_{1z} &= F_{1fy} \cdot l_{1CoG} - F_{1ry} \cdot (L_1 - l_{1CoG}) - P_{1cy} \cdot (l_{1c} - l_{1CoG}) \end{aligned} \tag{1}$$

The compatibility equations are derived as:

$$\begin{aligned} v_{1fy} &= v_{1y} + \omega_{1z} \cdot l_{1CoG}, & v_{1fxw} &= v_{1x} \cdot \cos\left(\delta_f\right) + v_{1fy} \cdot \sin(\delta_f) \\ v_{1ry} &= v_{1y} - \omega_{1z} \cdot (L_1 - l_{1CoG}), & v_{1fyw} &= -v_{1x} \cdot \sin(\delta_f) + v_{1fy} \cdot \cos\left(\delta_f\right) \end{aligned} \tag{2}$$

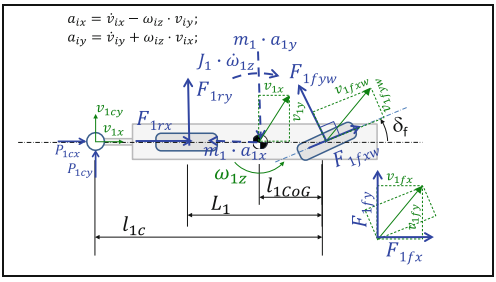

Fig. 1. Free body diagram of the tractor

The lateral axle slips and the lateral tire forces are defined as:

$$s_{1fy} = \frac{v_{1fyw}}{|v_{1fxw}|}, \; s_{1ry} = \frac{v_{1ry}}{|v_{1x}|} \tag{3}$$

$$F_{1fyw} = -C_{1f} \cdot s_{1fy} \cdot F_{1fz}, \; F_{1ry} = -C_{1r} \cdot s_{1ry} \cdot F_{1rz} \tag{4}$$

Here, the tractor yaw acceleration, $\dot{\omega}_{1z}$, is assumed to be zero for model simplicity. As longitudinal speeds are always positive, the absolute signs in (3) are omitted. All longitudinal wheel forces are set to zero, meaning the reference side-slip angle is calculated for a quasi steady-state turning maneuver without braking or propelling. The longitudinal vehicle speed, v_{1x}, and the steering angle, δ_f, are known inputs to the estimator. Furthermore, the lateral coupling force, P_{1y}, is considered known, simplifying the estimator and avoiding the semitrailer equations. A total of 10 equations can be solved for 10 unknowns: $\omega_{1z}, F_{1fyw}, F_{1ry}, s_{1fy}, s_{1ry}, v_{1fyw}, v_{1ry}, v_{1fxw}, v_{1fy}, v_{1y}$. The vehicle parameters are given in Table 1. This open-loop estimator calculates the reference lateral axle slip, s_{1ry}, as a side-slip angle (β^{ref}) at the tractor drive axle. Its accuracy, validated against VTM (Volvo Transport Model) high-fidelity model [7] simulations, reaches approximately $\pm\, 0.1°$ for various maneuvers.

Table 1. Tractor vehicle parameters for reference side-slip angle estimation

Parameter	Explanation	Value	Unit
F_{1fz}, F_{1rz}	Front and rear axle normal loads	67689, 91741	N
C_{1f}, C_{1r}	Normalized front and rear axle cornering stiffnesses	6	N/N/rad
L_1	Tractor wheelbase	3.8	m
l_{1CoG}, l_{1c}	Tractor CoG and coupling distance to the front axle	1.351, 3.225	m
m_1	Tractor mass	9000	kg

3 Simulation Tests

In this section, the performance of two slip controllers are compared: one with a fixed longitudinal slip limit and another one with an adaptive longitudinal slip limit based on the side-slip angle, using the VTM. In the first controller, S_x^{lim} is set at + 10% for propulsion and −7.5% braking. In the second controller, S_x^{lim} decreases for any deviation from β^{ref} (estimated via the estimator explained in Sect. 2), on the tractor drive axle, as shown in Fig. 2. S_x^{lim} is linearly decreased and set as 0 for ± 1° deviation from β^{ref}. This would provide more lateral force capability for the tires to maintain yaw stability at high side-slip angles and high lateral accelerations. The resultant shape of the slip limits is a 2-dimensional polytope.

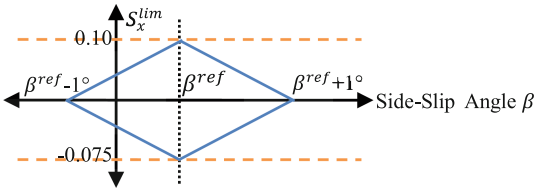

Fig. 2. Tractor EM slip limit. Case a: fixed (orange), Case b: adaptive (blue).

β^{ref} is estimated using the estimator for a quasi-steady-state maneuver as explained in Sect. 2. Inputs to the estimator, (v_{1x}, δ_f, and P_{1y}), are extracted from the VTM model. Figure 3 illustrates a propel-in-turn maneuver performed on ice (with 0.1 friction coefficient, μ) on a reference path with a 115 m turning radius. The vehicle combination accelerates to 25 km/h with a rather low, 40% friction utilization (3670 N axle force). Here, the friction utilization is defined as $F_x/(\mu F_z)$, where the F_x and F_z are the longitudinal and normal forces on the wheels. When the vehicle reaches 25 km/h (indicated by a black vertical line), the tractor drive axle propulsion forces are increased from 3670 N to 9170 N, reaching full (100%) friction utilization. Slip controllers control wheel slips, with one EM equipped with a slip controller per driven wheel. A simple PID controller for path-following steers the vehicle. The vehicle equipped with a fixed slip limit controller (case a) experiences jackknifing, with the speed, V_x reaching a maximum of 26.3 km/h. The vehicle equipped with more advanced slip controller with an adaptive S_x^{lim} (case b),

on the other hand, can accelerate smoothly and stably up to 34 km/h. During maneuver b, longitudinal slip, S_x; side-slip angle, β; and steering wheel angle, δ, are kept at reasonable values.

In Table 2, simulation results for four maneuvers are presented, comparing constant and adaptive slip limits. Previous results are related to maneuver 1. Two friction coefficients are tested: $\mu = 0.1$ for ice, and $\mu = 0.3$ for snow. Four turning radii, R, with various initial speeds, $V_{initial}$, and target speeds, V_{target}, are examined. $V_{initial}$ is the speed at which the longitudinal force corresponding to full friction utilization is applied, indicated by solid vertical lines in Fig. 3. In Table 2, additionally, normalized lateral acceleration values, $\frac{V_{target}^2/R}{\mu \cdot g}$, for the given friction coefficients and turning radii, are included. These values, ranging between 0.7 and 0.8 for all maneuvers, signify the aim for high lateral accelerations by the end of the maneuvers.

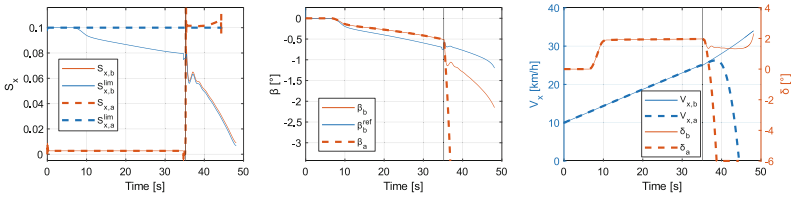

Fig. 3. Simulated test state plots for constant (a) and adaptive (b) slip limits

Table 2. Simulation test results

Maneuver	μ	R [m]	$V_{initial}$ [km/h]	V_{target} [km/h]	$\frac{V_{target}^2/R}{\mu \cdot g}$	a: Constant S_x^{lim}		b: Adaptive S_x^{lim}	
						V_{max} [km/h]	Jack-knifing	V_{max} [km/h]	Jack-knifing
1	0.1	115	25	34	0.79	26.3	Yes	34.0	No
2	0.1	160	30	40	0.79	31.1	Yes	40.0	No
3	0.3	70	35	44	0.73	37.5	Yes	44.0	No
4	0.3	137.5	50	61	0.71	52.0	Yes	61.0	No

All maneuvers employing slip controllers with fixed slip limits result in jackknifing, with the vehicle's maximum reachable speed, V_{max}, only a few km/h higher than $V_{initial}$. This indicates that applying a high propulsion force with a fixed slip limit on the slip controller leads to instability and jackknifing, as shown in the path plots in Fig. 4. Conversely, the vehicle equipped with slip controllers with adaptive slip limits can reach V_{target}, without encountering stability problems.

4 Real Vehicle Tests

The test vehicle accelerates from 25 km/h to 40 km/h on an ice surface ($\mu \approx 0.1$) along a circular track with a radius of 115 m, with a high propulsion force corresponding to full friction utilization. The slip controller for the tractor's EM is activated, while the electronic stability controllers are turned off. Side-slip angles are accurately measured using a global navigation satellite system/inertial navigation system.

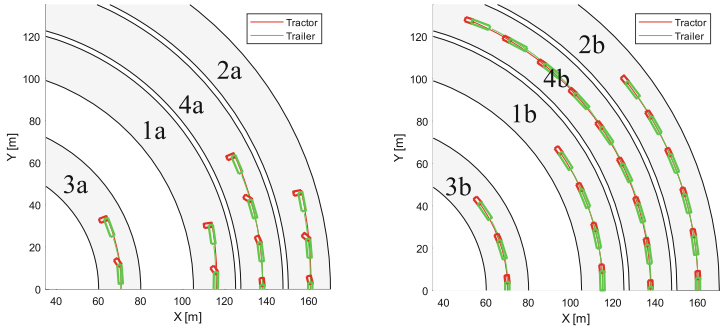

Fig. 4. Path plots of the maneuvers

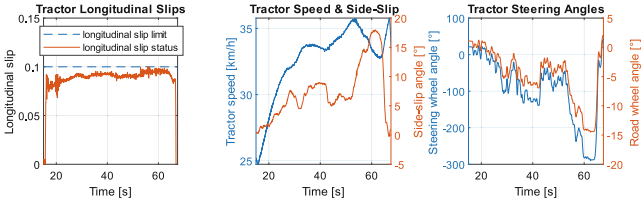

Fig. 5. State plots for real vehicle test with default slip controller

With the default slip controller (constant 10% slip limit), depicted in Figs. 5 and 7, the longitudinal slips remain under 10%. However, despite significant counter-steering effort by the driver (up to -15° road wheel angle), the side-slip angle grows to significant values (up to 18°). The vehicle fails to accelerate up to 40 km/h even in 53 s. The vehicle motion is quite unstable and always has large yaw dynamics.

The test results with the adaptive slip limit are shown in Figs. 6 and 7. β^{ref} is set at $+$ 1°, which represents the observed quasi-steady-state β for the maneuver, without using the β^{ref} estimator as in the simulated tests. However, the side-slip angle margin remains at $\pm$ 1°, consistent with the simulated tests. With this strategy, the vehicle reaches a speed of 40 km/h in just 17 s, as shown in Fig. 6. Moreover, this is achieved with minimal side-slip angles (always below 2°) and without requiring additional driver counter-steering effort from the driver. The driver can easily follow the lane with a very reasonable (approximately) 1.5° road wheel angle.

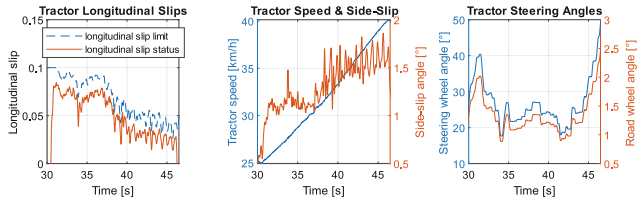

Fig. 6. State plots for real vehicle test with slip controller with adaptive slip limits

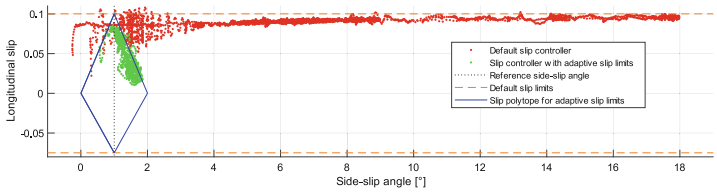

Fig. 7. Longitudinal slip vs. side-slip angle scatter plot for two types of controllers

5 Conclusion

This study introduces a side-slip angle estimator and a slip controller incorporating an adaptive longitudinal slip limit based on lateral slip and compares it against the default slip controller through both simulations and real vehicle tests. Simulation results demonstrate the superior performance of adaptive slip limits over fixed slip limits for various maneuvers on ice and snow, and for different turning radii. In real tests, the superior performance of the adaptive slip limits is validated when the driver is in the loop. The study shows that adaptive slip limits not only ensure yaw stability but also improve acceleration performance. The slip polytope used in this study is two-dimensional, constraining longitudinal slip as a function of the tractor's side-slip angle. However, it is envisioned that the polytope can have more dimensions, such as side-slip angles of the trailing units, and yaw rates. A reference side-slip angle estimator for a well-performing quasi-steady-state turning maneuver is presented. Additionally, this estimator can also estimate the reference yaw rate, which can be employed in the safety polytope. A significant advantage of this method is that friction estimation is not required although it could improve the reference side-slip angle estimator. Even though this paper focuses on a tractor and a semitrailer combination, the adaptive slip limits are applicable to passenger cars and single unit heavy vehicles as well.

References

1. Erdinc, U., Jonasson, M., Kati, M.S., et al.: Safe operating envelope based on a single-track model for yaw instability avoidance of articulated heavy vehicles. Veh. Syst. Dyn. (2023). https://doi.org/10.1080/00423114.2023.2276767
2. Erdinc, U., Jonasson, M., Kati, M.S., et al.: Validation of high-fidelity simulation-based safe operating envelopes for articulated heavy vehicles using real test data. Veh. Syst. Dyn. (2024). https://doi.org/10.1080/00423114.2023.2296595
3. Fu, R., Zhang, H., Guo, Y., et al.: Real-time estimation and prediction of lateral stability of coaches: a hybrid approach based on EKF, BPNN, and online autoregressive integrated moving average algorithm. IET Intell. Transp. Syst. **14**(13), 1892–1902 (2020). https://doi.org/10.1049/iet-its.2020.0385
4. Funke, J., Brown, M., Erlien, S.M., et al.: Collision avoidance and stabilization for autonomous vehicles in emergency scenarios. IEEE Trans. Control Syst. Technol. **25**(4), 1204–1216 (2017). https://doi.org/10.1109/TCST.2016.2599783
5. Erlien, S.M., Fujita, S., Gerdes, J.C.: Shared steering control using safe envelopes for obstacle avoidance and vehicle stability. IEEE Trans. Intell. Transp. Syst. **17**(2), 441–451 (2016). https://doi.org/10.1109/TITS.2015.2453404

6. Jacobson, B.J.H.: Vehicle Dynamics Compendium. Chalmers University of Technology, Gothenburg (Sweden) (2020)
7. Fröjd N. Handling analysis and control development of commercial trucks with Volvo Transport Models. Material presented at: MATLAB EXPO 2021; 2021 May 4–5. Available from: https://se.mathworks.com/videos/handling-analysis-and-control-development-of-commercial-trucks-with-volvo-transport-models-1622035211192.html